Electronic Supplementary Material (ESI) for Nanoscale.

Direct visualization of carbon nanotube degradation in primary cells by photothermal imaging

Julie Russier,[1] Laura Oudjedi,[2,3] Martin Piponnier,[2,3]

Cyrill Bussy,[4] Maurizio Prato,[5,6,7] Kostas Kostarelos,[4] Brahim Lounis,[2,3] Alberto Bianco,[1]*

Laurent Cognet[2,3]*

[1] University of Strasbourg, CNRS, Immunopathology and therapeutic chemistry, UPR 3572, 67000 Strasbourg, France

[2] University of Bordeaux, LP2N, F-33405 Talence, France

[3] Institut d'Optique & CNRS, LP2N, F-33405 Talence, France

[4] Nanomedicine Laboratory, Faculty of Biology, Medicine and Health and National Graphene Institute, University of Manchester, AV Hill Building, Manchester M13 9PT, United Kingdom

[5] Dipartimento di Scienze Chimiche e Farmaceutiche, Università di Trieste, Trieste 34127, Italy

[6] Carbon Nanobiotechnology Laboratory, CIC biomaGUNE, Paseo de Miramón 182, 20009 Donostia-San Sebastian (Spain)

[7] Basque Fdn Sci, Ikerbasque, Bilbao 48013, Spain

SUPPORTING INFORMATION

Material and methods

Functionalization of carbon nanotubes. MWCNTs were purchased from Nanostructured & Amorphous Materials Inc. (NanoAmor, Regular MWCNTs 95% pure, stock No. 1240XH). Outer average diameter was between 20 and 30 nm, and length between 0.5 and 2 µm. Pristine MWCNTs were functionalized by 1,3-dipolar cycloaddition. [1-3] Briefly, functionalization was achieved by treating pristine nanotubes with azomethine ylides generated *in situ* from the condensation of a α-amino acid and paraformaldehyde at reflux in DMF. The resulting pyrrolidine rings introduced on the nanotube surface bear a primary amine function at the end of the triethylene glycol chain, blocked by a protecting group (Boc). Removal of this protecting group in acidic conditions allows obtaining ammonium-functionalized MWCNTs (MWCNT-NH_3^+).[1-3]

Microglial cells

The preparation of primary microglia enriched cell cultures were performed as previously reported,[4]and according to a previously described method, based on mild trypsinisation of mixed glial cell culture prepared from rat embryonic stratial extracts.[5] Microglia enriched cell cultures were then exposed for 2 h to a non-cytotoxic 10 µg/mL CNT suspension prepared in serum free cell culture medium (DMEM:F12 medium). After 2 h incubation at 37°C without serum, the cell culture medium was completed with heat inactivated foetal bovine serum (12%). After 24 h incubation at 37°C, the supernatant containing CNTs was removed, cells were washed twice with pre-warmed PBS and then incubated with CNT free complete medium (DMEM:F12 with 12% serum) for 1, 7, and 14 days (recovery period). CNT-free complete medium was changed every 3 days.

Sample preparation

At the end of incubation time (1, 7 and 14 days), cells cultured on glass coverslip were washed with Tris buffer saline (TBS) and fixed overnight at 4 °C with 4 % glutaraldehyde. On the following day, cells were washed twice in distilled water and then submitted to a secondary fixation with 1% aqueous osmium tetroxide (30 min at room temperature). After rinsing cells three times with distilled water, dehydratation was performed through a series of baths: twice with 50% ethanol (10 min), once with 70% ethanol (20 min), once with ethanol 95% (10 min), twice with absolute ethanol (10 min) and finally twice with propylene oxide (for 10 min each). Infiltration with epoxy resin Epon was done using mixtures of propylene oxide and Epon resin in 2:1 (1 h) and 1:2 (1 h) ratio and finally with pure resin (1 h). On the last day, resin was replaced with fresh one and further incubated during three hours. Polymerized block with

embedded cells were then prepared filling BEEM® embedding capsules with fresh resin and placing them upon the glass coverslips on which cells were grown. The as prepared capsules were then placed into the oven to polymerize the resin at 60 °C for 48 h. Afterwards, glass coverslips were removed from the polimerized block surface and semi-thin sections (500 nm thick) were obtained using an ultramicrotome (Leica) with a glass knife. Semi-thin sections were then collected on glass slides, mounted in DAKO and observed by PhI.

Photothermal imaging

The principle of PhI has been described elsewhere.[6] In brief, the setup used in this study consists of a probe beam (HeNe laser, 633 nm, power of ~ 0,5 mW at the sample) overlaid with a cw absorption beam which intensity is modulated at 700 kHz (frequency-doubled YAG laser, 532 nm) (Figure S1). The absorption and probe beams were both focused onto the sample using a high NA objective (60×, NA=1,49). The absorption beam was circularly polarized and had an intensity of ~ 200 kW/cm^2 at the sample. The probe-transmitted and probe-scattered fields were collected by a second objective (60×, NA=1,0) and focused on a fast photodiode, connected to a lock-in amplifier to extract their beat signal at the modulating frequency.[6] The sample was mounted on a piezo-scanner stage that allowed scanning the sample to acquire 2D images. All data where acquired with integration times of 5 ms/pixel using a resolution of 150 nm/pixel.

Analysis of the PhI data

In each image, thresholding was used to extract PhI signals originating from CNTs from background signals in the following way. Histograms of signals from all pixels of the images systematically revealed the presence of three signal populations: a first population due to background noise, a second population due to background signals of the cells independent from CNT signals and a third population due to CNTs. Each image was then binarized by applying a global threshold so that pixels with background noise and cell signals were below the threshold and pixels containing CNT signals were selected. On the binary images, we then applied a connected components algorithm to isolate the areas corresponding to isolated or aggregated CNTs. For each area, the surface was measured in arbitrary units normalized to one for the point-spread-function of the microscope. Areas with surfaces significantly smaller than the point-spread-function were discarded considering that they were due to background noise not filtered during the thresholding process. The point-spread-function of the microscope, primarily given by the product of the (absorption and probe) focused beam spatial distributions,[6] was measured by imaging 10 nm individual gold nanoparticles acting as punctual absorbers (not shown), and was of the order of 290 nm. Cumulative histograms of the surface areas measured for day 1, day 7 and day 14 are presented in Figure 3A. For each isolated area, we

also calculated the signal intensity defined as the sum of all pixel values inside the area normalized by the surface area. Cumulative histograms of the signal intensities are presented in Figure 3B.

Scheme of the PhI microscope

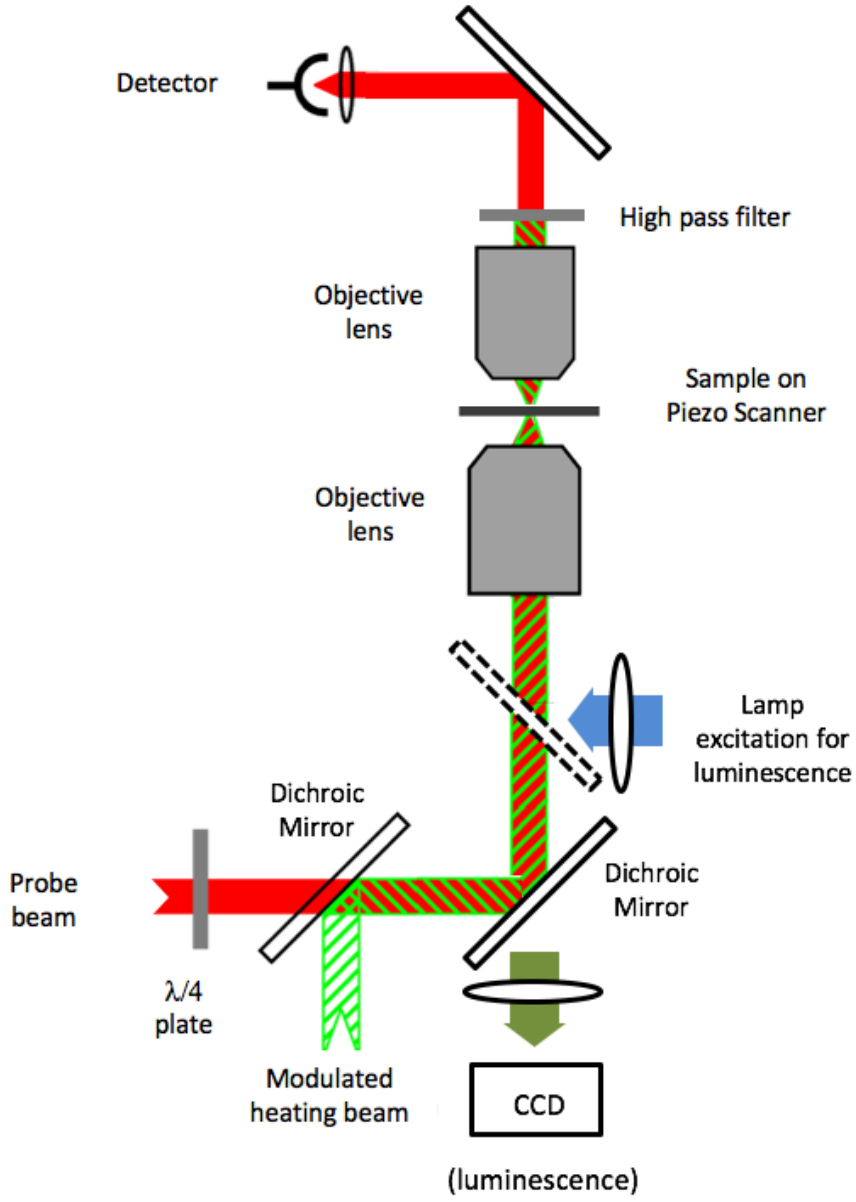

Figure S1. Experimental setup for PhI microscopy equipped with wide-field luminescence imaging by optional insertion of the dichroic mirror (dashed line).

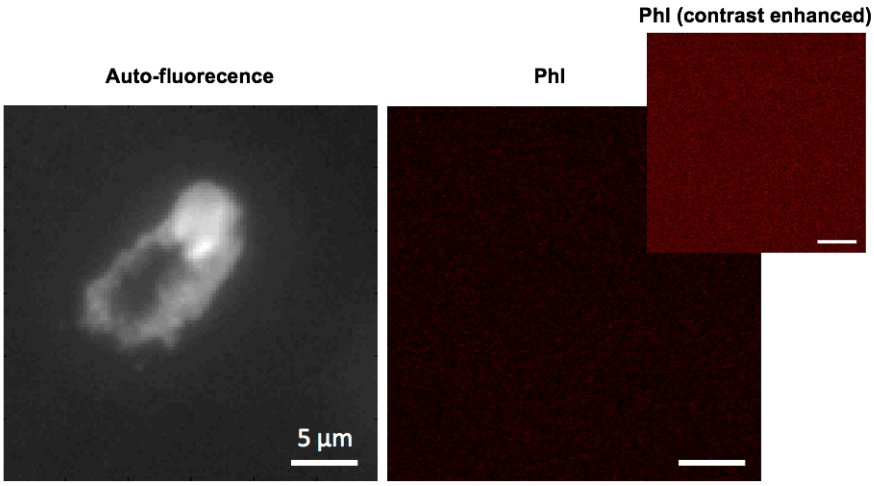

Figure S2. Negative control of Figure 2: Photoluminescence (left) and PhI images (right) of 500 nm semi-thin sections of resin embedded microglial cells that were not incubated with MWCNT-NH_3^+. Note that in the large PhI image, the same color scale was used as in Figure 2, and in the small image, an enhanced scaling is shown revealing the absence of weak signals.

Calibration of PhI point-spread-function

A dilute sample of 10 nm gold nanoparticles was spin-coated on the surface of plasma cleaned glass slides. A drop of silicon oil was then added on the sample to ensure homogenous heat diffusion. Images of the individual gold nanoparticles were detected by PhI as in Figure S3, and the dimension of the point-spread function of the PhI microscope was determined from the analysis of the spatial dimension of the images of these nanoscale absorbers. We find a mean point-spread function of 291± 13 nm (full-width-at-half maximum ± standard deviation, N=15).

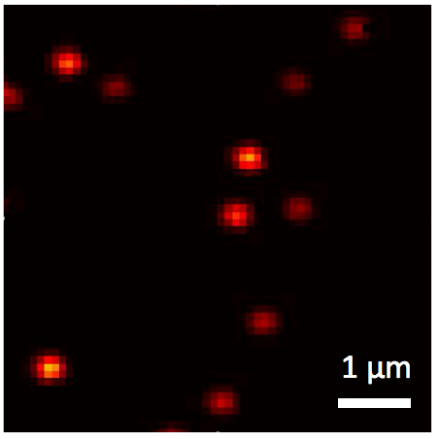

Figure S3. PhI images of 10 nm gold nanoparticles spin coated on a glass coverslip. Pixel size 100 nm.

Statistical information

Nine images were analyzed for day 1 corresponding to N = 131 segmented areas, six images for day 7 corresponding to N = 119 segmented areas and ten images for day 14 corresponding to N = 334 segmented areas.

References

1 A. Nunes, C. Bussy, L. Gherardini, M. Meneghetti, M. A. Herrero, A. Bianco, M. Prato, T. Pizzorusso, K. T. Al-Jamal and K. Kostarelos, *Nanomedicine (Lond)*, 2012, **7**, 1485–1494.

2 H. Ali-Boucetta, A. Nunes, R. Sainz, M. A. Herrero, B. Tian, M. Prato, A. Bianco and K. Kostarelos, *Angew. Chem. Int. Ed.*, 2013, **52**, 2274–2278.

3 V. Georgakilas, N. Tagmatarchis, D. Pantarotto, A. Bianco, J.-P. Briand and M. Prato, *Chem. Commun.*, 2002, 3050–3051.

4 C. Bussy, C. Hadad, M. Prato, A. Bianco and K. Kostarelos, *Nanoscale*, 2016, **8**, 590–601.

5 J. Saura, J. M. Tusell and J. Serratosa, *Glia*, 2003, **44**, 183–189.

6 S. Berciaud, D. Lasne, G. A. Blab, L. Cognet and B. Lounis, *Phys. Rev. B*, 2006, **73**, 045424.